IOP Publishing

Fast Track Communications
Journal of Physics: Condensed Matter

J. Phys.: Condens. Matter **26** (2014) 502101 (6pp)
doi:10.1088/0953-8984/26/50/502101

Fast Track Communication

Nonlocal thermal transport across embedded few-layer graphene sheets

Ying Liu[1], Scott T Huxtable[1], Bao Yang[2], Bobby G Sumpter[3] and Rui Qiao[1]

[1] Department of Mechanical Engineering, Virginia Tech, Blacksburg, VA 24061, USA
[2] Department of Mechanical Engineering, University of Maryland, College Park, MD 20742, USA
[3] Center for Nanophase Materials Science and Computer Science & Mathematics Division, Oak Ridge National Laboratory, Bethel Valley Road, Oak Ridge, TN 37831-6367, USA

E-mail: ruiqiao@vt.edu

Received 19 August 2014, revised 24 September 2014
Accepted for publication 17 October 2014
Published 13 November 2014

Abstract

Thermal transport across the interfaces between few-layer graphene sheets and soft materials exhibits intriguing anomalies when interpreted using the classical Kapitza model, e.g. the conductance of the same interface differs greatly for different modes of interfacial thermal transport. Using atomistic simulations, we show that such thermal transport follows a nonlocal flux-temperature drop constitutive law and is characterized jointly by a quasi-local conductance and a nonlocal conductance instead of the classical Kapitza conductance. The nonlocal model enables rationalization of many anomalies of the thermal transport across embedded few-layer graphene sheets and should be used in studies of interfacial thermal transport involving few-layer graphene sheets or other ultra-thin layered materials.

Keywords: interfacial thermal transport, soft materials, layered materials, nonlocal transport

S Online supplementary data available from stacks.iop.org/JPhysD/47/502101/mmedia

(Some figures may appear in colour only in the online journal)

Heat conduction across the interfaces between two materials is often accompanied by a finite temperature jump ΔT. The Kapitza model $q'' = G_k \Delta T$ (q'': heat flux; G_k: Kapitza conductance) is used universally to describe such interfacial transport [1–3]. Because interfacial thermal transport plays a key role in determining the performance of many nanodevices and nanomaterials, it has been studied extensively [4–8]. The majority of the prior work has focused on the thermal transport across the interfaces between bulk materials, including the use of methods such as lattice dynamics, Green's function techniques, and molecular dynamics (MD) [9–16]. Such transport is now understood reasonably well [2, 17]. Recently, few-layer graphene sheets have emerged as promising new thermal materials due to their superior thermal properties [18–20]. The thermal transport across their interfaces with other materials has been studied intensively [13, 21–25], and intriguing anomalies are emerging. Specifically, MD simulations showed that G_k of similar interfaces can range from 20 to 170 MW m^{-2} K^{-1} depending on the method used to compute it (see table 1) [9–11, 13, 14]. Recently, we showed that G_k between single-layer graphene sheets and oils depends on the modes of thermal transport: when heat enters a graphene sheet from one side of its basal plane and leaves through the other side (termed 'across' mode), the corresponding G_k is $\sim$150 MW m^{-2} K^{-1}; when heat enters/leaves a graphene sheet simultaneously from both sides of its basal plane (termed 'non-across' mode), the corresponding G_k is $\sim$5 MW m^{-2} K^{-1} [10]. These anomalies have been attributed to the resistance between the different phonon modes within graphene sheets [3, 9, 10] and the correlations between the thermal transport at a graphene sheet's two sides [10]. These useful insights, however, have not provided a quantitative model for the

Table 1. Thermal conductance of graphene–soft material interfaces reported in the literature.

Mode of interfacial thermal transport probed	G ($MW\,m^{-2}\,K^{-1}$)	System	Method	Ref.
'Across' mode	170 ± 20	2-layer graphene in phenolic resin	Place heat sources/sinks into the soft matrix to generate an overall heat flux normal to the graphene sheet's basal plane; measure the temperature drop at graphene–matrix interfaces	[9]
	142 ± 4 [a]	Single-layer graphene in paraffin wax	Same as above	[11]
	150 ± 15.3	Single-layer graphene in octane	Same as above	[10]
'Non-across' mode	21	3-layer graphene in phenolic	Thermal relaxation method [26]	[9]
	20	3-layer graphene in phenolic	Place a heat source on the graphene and a heat sink in the soft material; measure the temperature drop at graphene–matrix interfaces	[9]
	18 ± 0.7	3-layer graphene in octane	Same as above	[13]
	30	Single-layer graphene in phenolic resin	Place a pair of heat sources/sinks into the soft matrix to generate an overall heat flux parallel to the graphene sheet's basal plane; extract G using an effective medium theory	[14]
	4.3 ± 0.44	Single-layer graphene in octane	Same as above except that G was extracted using a one-dimensional model	[10]

[a] In this paper, a G of $71 \pm 2\,MW\,m^{-2}\,K^{-1}$ was obtained for two graphene–polymer interfaces formed by a single graphene layer immersed in polymeric resins.

interfacial thermal transport. As such, the Kapitza model is used universally despite the above anomalies. More generally, the fact that G_k of an interface depends very strongly on how thermal transport at the interface is probed (i.e., the 'mode' of interfacial thermal transport), is conceptually undesirable—G_k should be a material property and thus independent of the mode of thermal transport. Therefore, there is a need to develop a better model for thermal transport at the interfaces between few-layer graphene sheets and bulk materials.

In this work, we examine the thermal transport across few-layer graphene sheets embedded in soft materials using MD simulations. We show that such thermal transport cannot be described by the Kapitza model even qualitatively. We then propose a nonlocal model for such transport. This model helps rationalize the anomalies of thermal transport across embedded few-layer graphene sheets and can be used in analysis of interfacial thermal transport involving few-layer graphene sheets and many other layered materials.

Anomalous interfacial thermal transport. Our MD system (see figure 1) features a two-layer graphene sheet embedded in octane fluids, whose thermal behavior is representative of soft materials. Graphene was modeled using the REBO potential [27]; octane fluids were modeled using the force fields in [28]. The graphene–graphene and graphene–octane interactions were modeled using the Lennard-Jones potential with parameters derived from the Lorentz–Berthelot rules. Using a different model for the graphene, [29] whose form differs greatly from that of the REBO potentials, gave very similar results.

We performed three sets of simulations using the LAMMPS code [30]. In the first set of simulations, we studied the thermal transport through graphene sheets in the 'across mode' *at steady state*. The system was first equilibrated in the NVT ensemble ($T = 300\,K$) for 2 ns and then in the NVE ensemble for 3 ns. These runs were followed by a production NVE run during which heat was added to (removed from) the heat source (sink) at $-7\,nm < x < -6\,nm$ ($13.5\,nm < x < 14.5\,nm$) by velocity rescaling [11] to create a heat flux across the system (see online figure S1(a)). In the second set of simulations, we studied the thermal transport through graphene in the 'non-across mode' at steady state. These simulations differ from the first set of simulations in that during the production run, (1) heat was added into the graphene sheets and removed from the two heat sinks located in $-7\,nm < x < -6\,nm$ and $6\,nm < x < 7\,nm$, and (2) octane molecules in the region $7\,nm < x < 14.5\,nm$ were fixed (see online figure S1(b)). From the steady-state temperature profiles of the octane fluids and the graphene sheet, G_k of the graphene–octane interface was computed using the Kapitza model. We obtained G_k of $128 \pm 14\,MW\,m^{-2}\,K^{-1}$ and $13 \pm 0.5\,MW\,m^{-2}\,K^{-1}$ for the 'across' and the 'non-across' modes of thermal transport, respectively. These values and their large difference are similar to those reported previously [9–11].

In the third set of simulations, we studied the thermal transport through graphene in the 'across mode' under *non-steady state* conditions. These simulations were the same as those in the first set of simulations except that, during the production run, which began at $t = 0$ and lasted for 500 ps, heat was added into the heat source at a constant rate but *not* removed from the heat sink (see online figure S1(c)). We studied the same problem using continuum models[4]. The temperature of the octane fluids, T_f, was modeled using $\partial T_f/\partial t = a_f \partial^2 T_f/\partial x^2$, where a_f is octane's thermal diffusivity. The graphene temperature, T_g, was modeled using $C_g \partial T_g/\partial t = q''_1 - q''_2$, where C_g is the

[4] See supplemental material (stacks.iop.org/JPCM/26/502101/mmedia) for simulation details and derivation of the intrinsically nonlocal interfacial thermal transport equations.

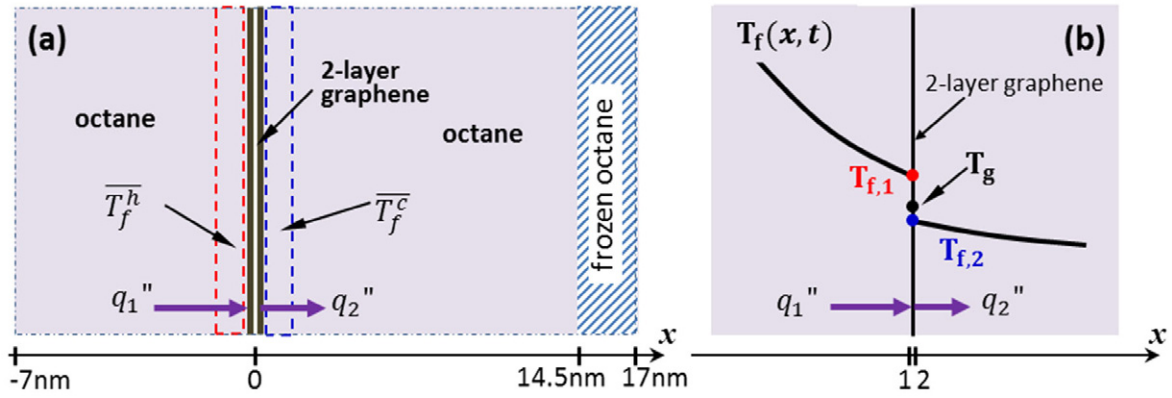

Figure 1. Schematics of the MD (*a*) and continuum (*b*) models used to study interfacial thermal transport across two-layer graphene sheets embedded in octane fluids. The MD system is periodic in all directions. The octane fluids and the graphene sheet have dimensions of $11.9 \times 11.8\,\mathrm{nm}^2$ in the *yz*-plane. The octane molecules in the region $14.5\,\mathrm{nm} < x < 17\,\mathrm{nm}$ are frozen to avoid thermal short-circuiting. The dashed boxes denote the observation windows (width: 1.1 nm) in which the average temperature of the octane fluids was monitored in non-steady simulations (see figure 2). $q''_{1,2}$ are the interfacial heat fluxes and $T_{f,1,2}$ are the temperatures of the octane near the two surfaces of the graphene sheet. In (*b*), '1' ('2') denotes the left (right) surface of the graphene sheet. For clarity, only the portion of the system near the graphene sheet is shown. To drive thermal transport in the system, a heat source and sink were introduced (see text and figure S1(*a*)–(*c*)).

graphene sheet's heat capacity, and q''_1 and q''_2 are the interfacial heat fluxes given by the Kapitza model (see figure 1(*b*)): $q''_1 = G_k(T_{f,1} - T_g)$, $q''_2 = G_k(T_g - T_{f,2})$, where $T_{f,1}$ and $T_{f,2}$ are the temperature of the octane fluids on the graphene sheet's two surfaces. The lumped treatment of the graphene sheet is consistent with the fact that the individual layers of the graphene sheet are in excellent thermal contact [31, 32]. In separate simulations, a_f and C_g at 300 K were determined to be $7.75 \times 10^{-8}\,\mathrm{m^2\,s^{-1}}$ and $2.07\,\mathrm{kJ\,kg^{-1}\,K^{-1}}$ (see online supplementary data), respectively. The former value is ~3% smaller than the experimental value [33]. The latter value agrees well with that reported in prior simulations [34]. To examine the interfacial thermal transport, we focus on the evolution of T_g and the average temperature of the octane fluids in the two windows located within 1.1 nm from each side of the graphene (hereafter denoted as $\bar{T}_f^h$ and $\bar{T}_f^c$, see figure 1(a)). Figure 2(*a*) compares the evolution of $\bar{T}_f^h$, $\bar{T}_f^c$, and T_g predicted by the MD and continuum models. Both models predict $\bar{T}_f^h$, $\bar{T}_f^c$, and T_g to rise with time. However, the MD simulation predicted $\bar{T}_f^c$ to rise as fast as or even faster than T_g, an anomaly that differs qualitatively from the continuum prediction. In the continuum models, thermal transport is a diffusive, local process. In response to the heat added into a heat source, the temperature of the heat conduction medium (octane fluids and graphene sheet) rises slower as we move away from the heat source. We can prove that simulations based on the Kapitza model cannot reproduce the anomaly revealed by MD simulations for any choice of G_k (see online supplementary data).

Nonlocal model. To rationalize the anomalies of interfacial thermal transport noted above, we replace the Kapitza model by a nonlocal constitutive law. For the interface sketched in figure 1(*b*),

$$q''_1 = G_{ql}\left(T_{f,1} - T_g\right) + G_{nl}(T_g - T_{f,2}) \qquad (1a)$$

$$q''_2 = G_{ql}\left(T_g - T_{f,2}\right) + G_{nl}(T_{f.1} - T_g) \qquad (1b)$$

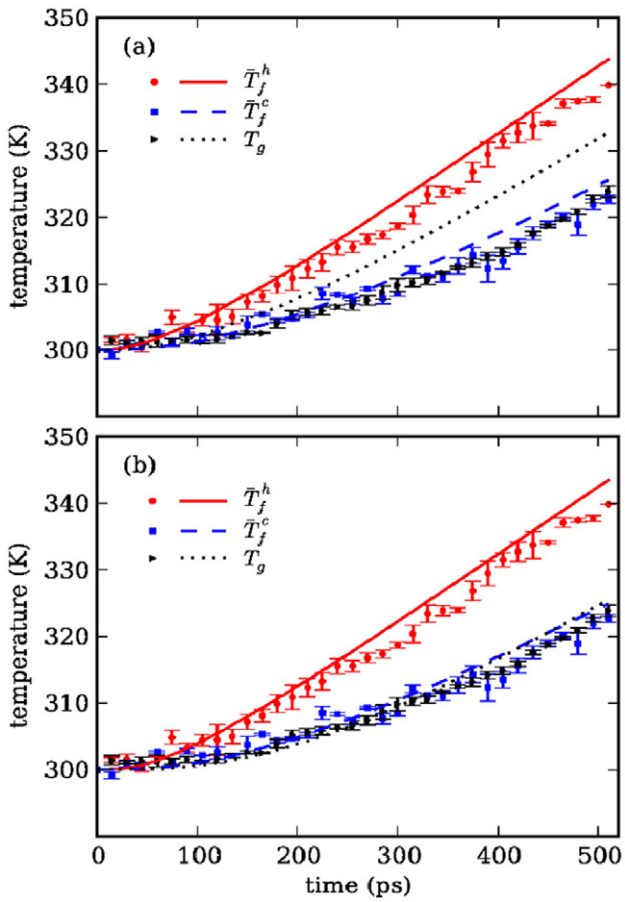

Figure 2. Evolution of the temperature of the graphene sheet and the octane fluids in the observation windows shown in figure 1(*a*) during the transient heating simulations described in the text. The predictions of the MD simulations (filled symbols) are compared with those by the continuum simulations (thin lines) based on the Kapitza model (*a*) and on the nonlocal model (*b*).

where G_{ql} and G_{nl} are the quasi-local and the nonlocal conductance, respectively. The idea is that the heat flux at interface '1' is partly driven by the temperature drop across

interface '2' and vice versa. To derive this model, we make two assumptions:

(1) *interfacial* thermal transport is dominated by the coupling between a small portion of the phonons in the graphene sheet (termed energy transport phonons) and the phonons in the fluids,
(2) the heat capacity of the energy transport phonons is small compared to the net heat capacity of other phonons in the graphene sheet (termed energy storage phonons).

These assumptions are reasonable for few-layer graphene sheets embedded in soft materials. Specifically, previous simulations indicated that the thermal transport across graphene–polymer interfaces is dominated by flexural (ZA) phonons with frequency lower than 4 THz [9]. Because of the strong sp^2 bonds, the in-plane vibration in graphene sheets is dominated by high-frequency longitudinal and transverse modes [10, 11]. These phonons and the high-frequency ZA phonons dominate graphene's heat capacity, thus justifying assumption (2). Denoting the temperature of the energy transport phonons and the energy storage phonons as $T_{g,et}$ and $T_{g,es}$, assumption (2) implies $T_g \approx T_{g,es}$. We introduce an internal conductance $G_i = q''_{et\to es}/[n(T_{g,et} - T_{g,es})]$ to describe the thermal transport from the energy transport phonons to the energy storage phonons in an n-layer graphene sheet, $q''_{et\to es}$. We introduce an external conductance $G_e = q''_1/(T_{f,1} - T_{g,et}) = q''_2/(T_{g,et} - T_{f,2})$ to describe the thermal transport between the graphene sheet's energy transport phonons and phonons of its surrounding fluids. Since assumption 2 implies that the energy accumulation in the energy transport phonons is negligible, we eliminate $T_{g,et}$ from q''_1 and q''_2, and obtain equations (1*a*) and (1*b*) with $G_{ql} = (nG_iG_e + G_e^2)/(nG_i + 2G_e)$ and $G_{nl} = G_e^2/(nG_i + 2G_e)$.

In the above derivation, the interfacial thermal transport is assumed to be intrinsically local, i.e., $q''_1 = (T_{f,1} - T_{g,et})G_e$. The non-locality of the overall thermal transport originates from the apparent absence of $T_{g,et}$ in equations (1*a*) and (1*b*). More fundamentally, the non-locality originates from the fact that, for few-layer graphene sheets embedded inside soft materials, the phonons that store most of the energy and the phonons that transport most of the energy reside in different parts of the spectrum and they are not in equilibrium. Such a separation of energy transport and storage phonons in solid materials has been shown to lead to nonlocal thermal transport involved in the transverse spin Seebeck effect [35].

It is possible that thermal transport through graphene–matrix interfaces is intrinsically nonlocal. We can derive a nonlocal constitutive law with a form that is the same as equations (1*a*) and (1*b*) (see online supplementary data) by postulating a nonlocal ansatz for q''_1 in the spirit of general nonlocal transport theories [36, 37] and prior works on nonlocal thermal transport [38, 39]. We cannot yet isolate this possible intrinsic nonlocal effect using simulations because eliminating nonlocal effects associated with the separation of energy transport and storage phonons within embedded graphene sheets is difficult.

The Kapitza conductance G_k can be related to G_{ql} and G_{nl} under special situations. The first situation is when $T_g = (T_{f,1} + T_{f,2})/2$, which was encountered in our first set of MD simulations described earlier. Here, the Kapitza model would predict the same thermal transport behavior as the nonlocal model if one sets $G_k = G_{ql} + G_{nl}$ because $q''_1 = G_{ql}(T_{f,1} - T_g) + G_{nl}(T_g - T_{f,2}) = (G_{ql} + G_{nl})(T_{f,1} - T_g)$. The second situation is when $T_{f,1} = T_{f,2}$, which is encountered in our second set of MD simulations. Here, for the Kapitza model to predict the same thermal transport behavior as the nonlocal model, one must set $G_k = G_{ql} - G_{nl}$ because $q''_1 = G_{ql}(T_{f,1} - T_g) + G_{nl}(T_g - T_{f,2}) = (G_{ql} - G_{nl})(T_{f,1} - T_g)$. For thin graphene sheets, $nG_i \ll G_e$ [9] and thus G_{nl} should be close to G_{ql} (see online supplementary data). Therefore, we expect that the apparent G_k of the same interface to be much smaller in the second situation than in the first situation, in agreement with our MD data. Clearly, adopting the nonlocal model helps explain this anomaly. The third situation is when $G_{nl} \ll G_{ql}$ (or equivalently, $nG_i/G_e \gg 1$), where we have $G_k \approx G_{ql}$ and the interfacial thermal transport is local. This situation is encountered in thick graphene sheets (see below).

Validation and applications of the nonlocal model. Beyond the situations presented above, it is difficult to relate G_k to G_{ql} and G_{nl}, and the Kapitza model may fail qualitatively. Then, the nonlocal model must be used to describe the interfacial thermal transport. Here we revisit the transient heating problem in figure 2(*a*) through new continuum simulations in which the Kapitza model is replaced by equations (1*a*) and (1*b*). To determine G_{ql} and G_{nl}, we used the following approach. Based on the apparent G_k determined in our first set of MD simulations, we obtained $G_{ql} + G_{nl} = 128\,\mathrm{MW\,m^{-2}\,K^{-1}}$. We next tuned G_{ql} and G_{nl} under this constraint to examine whether our new continuum simulation can reproduce the evolution of $\bar{T}_f^h$, $\bar{T}_f^c$, and T_g predicted by MD simulations. Figure 2(*b*) shows that, with $G_{ql} = 72.3\,\mathrm{MW\,m^{-2}\,K^{-1}}$ and $G_{nl} = 55.7\,\mathrm{MW\,m^{-2}\,K^{-1}}$, the continuum simulation reproduced the anomaly that $\bar{T}_f^c$ and T_g rises at nearly the same speed or even faster, which is not captured by simulations based on the Kapitza model. The fact that $\bar{T}_f^c$ rises as fast as (or faster than) T_g is caused by (1) the good coupling between the energy transport phonons in the graphene sheet with surrounding fluids which allow heat that is transmitted to the energy transport phonons by fluids at the hot side to pass to the fluids at the cold side easily (thus $\bar{T}_f^c$ rises quickly) and (2) the poor coupling between the energy transport and storage phonons in the graphene sheet which hinders the transport of heat from the energy transport phonons to energy storage phonons (thus T_g rises slowly). Note that the G_{ql} and G_{nl} fitted above gives a G_e of $128\,\mathrm{MW\,m^{-2}\,K^{-1}}$ (a G_i of $19.1\,\mathrm{MW\,m^{-2}\,K^{-1}}$), which is consistent with good (poor) coupling between the energy transport phonons and the phonons of the surrounding fluids (the energy storage phonons of the graphene sheet). Hence the above effects are incorporated in the nonlocal model, which helps capture the key features of the temporal evolution of $\bar{T}_f^h$, $\bar{T}_f^c$, and T_g. As a side note, using the G_e and G_i fitted above, we expect $G_{nl} \ll G_{ql}$ to hold (i.e., the interfacial thermal transport becomes local) only when there are at least tens of layers in the graphene sheet.

A more stringent test of the model is to check whether the transport properties obtained for a graphene–octane interface

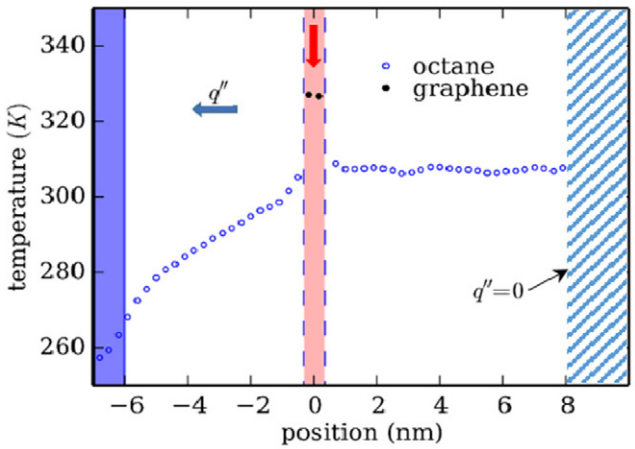

Figure 3. Temperature profiles of the octane fluids and the graphene sheet shown in figure 1. Heat is injected into the graphene sheet and removed from the octane fluids in the purple shaded region ($-7\,\text{nm} < x < -6\,\text{nm}$). The two vertical dashed lines denote the two surfaces of the graphene sheet.

in one transport mode can be used to predict the thermal transport in other modes, for which the Kapitza model fails. To this end, recall that the nonlocal model predicts that the apparent Kapitza conductance of a graphene–octane interface is $G_k = G_{ql} - G_{nl}$ for the interfacial thermal transport examined in the second set of simulations (i.e., the 'non-across mode' at steady state). With the G_{ql} and G_{nl} fitted above, the nonlocal model predicts an apparent G_k of 16.6 MW m^{-2} K^{-1}, which compares well with the 13.0 MW m^{-2} K^{-1} measured in MD simulations.

The nonlocal model also predicts other interesting phenomena. In the system shown in figure 1, we injected heat into the graphene sheets and removed heat from a heat sink located at the left side of the graphene sheet to generate a heat flux of $q'' = 500\,\text{MW m}^{-2}\,\text{K}^{-1}$ from the graphene sheets to the heat sink (see figure 3). The Kapitza model predicts that the temperature of the graphene sheet is the same as that of the octane fluids at its right side, $T_{f,R}$, i.e., $T_g = T_{f,R}$. The nonlocal model predicts that $T_g - T_{f,R} = q''G_{nl}/(G_{ql}^2 - G_{nl}^2)$. Using the G_{ql} and G_{nl} extracted above, we obtained $T_g - T_{f,R} = 13.1$ K, which agrees reasonably well with the MD result of 18.9 ± 1.1 K. To understand this phenomenon, we note that heat was injected into the graphene sheet through velocity rescaling. Hence most of the heat was injected into the high-frequency phonons (i.e., the energy storage phonons) [9]. Because of the small conductance between the energy storage and transport phonons, the temperature of the energy storage phonons is much higher than that of the energy transport phonons. The temperature of the graphene sheet is close to that of its energy storage phonons due to their large heat capacity. Since the energy transport phonons of the graphene sheet are in good equilibrium with the octane fluids at *both* sides, it follows that the temperature of the graphene sheet is higher than the octane fluids at both sides.

In summary, we proposed a nonlocal model for the thermal transport across few-layer graphene sheets embedded in soft materials. The model provides a more coherent description of the interfacial transport compared to the Kapitza model by characterizing such transport using a pair of conductances that are independent of the mode of thermal transport. The model is useful for interpreting experimental measurements of interfacial thermal conductance and could replace the Kapitza model, which, despite the recognition of its many potential limitations/anomalies [3], is used universally because of the lack of a more effective model.

The non-locality of the interfacial thermal transport across graphene sheets embedded in soft materials originates from the properties that the energy transport and storage phonons are separated (with respect to frequency) and not in equilibrium. Since these properties are generic to thin, layered materials in which atoms of the same layer are strongly bonded (e.g. boron nitride and dichalcogenide sheets), the nonlocal model should be applicable to these materials. Validating the applicability of the nonlocal model for these thin layered materials and leveraging its predictions may create new opportunities for controlling thermal transport across interfaces.

Acknowledgments

The authors thank the CCIT at Clemson University and the ARC at Virginia Tech for generous allocation of computing time. BY and RQ gratefully acknowledge support from NSF. RQ was partially supported by an appointment to the HERE program for faculty at the Oak Ridge National Laboratory (ORNL) administered by ORISE. BGS acknowledges the support from the Center for Nanophase Materials Sciences, which is sponsored at ORNL by the Scientific User Facilities Division, Office of Basic Energy Sciences, US Department of Energy.

References

[1] Chen G 2005 *Nanoscale Energy Transport and Conversion: A Parallel Treatment of Electrons, Molecules, Phonons, and Photons* (Oxford: Oxford University Press)
[2] Swartz E T and Pohl R O 1989 Thermal boundary resistance *Rev. Mod. Phys.* **61** 605
[3] Cahill D G *et al* 2014 Nanoscale thermal transport: II. 2003–2012 *Appl. Phys. Rev.* **1** 011305
[4] Cahill D G, Ford W K, Goodson K E, Mahan G D, Majumdar A, Maris H J, Merlin R and Phillpot S R 2003 Nanoscale thermal transport *J. Appl. Phys.* **93** 793–818
[5] Ge Z, Cahill D G and Braun P V 2006 Thermal conductance of hydrophilic and hydrophobic interfaces *Phys. Rev. Lett.* **96** 186101
[6] Barrat J and Chiaruttini F 2003 Kapitza resistance at the liquid–solid interface *Mol. Phys.* **101** 1605
[7] Harikrishna H, Ducker W A and Huxtable S T 2013 The influence of interface bonding on thermal transport through solid–liquid interfaces *Appl. Phys. Lett.* **102** 251606
[8] Yang B and Chen G 2003 Partially coherent phonon heat conduction in superlattices *Phys. Rev.* B **67** 195311
[9] Hu L, Desai T and Keblinski P 2011 Determination of interfacial thermal resistance at the nanoscale *Phys. Rev.* B **83** 195423
[10] Liu Y, Huang J, Yang B, Sumpter B G and Qiao R 2014 Duality of the interfacial thermal conductance in graphene-based nanocomposites *Carbon* **75** 169–77

[11] Luo T and Lloyd J R 2012 Enhancement of thermal energy transport across graphene/graphite and polymer interfaces: a molecular dynamics study *Adv. Funct. Mater.* **22** 2495–502
[12] Young D A and Maris H J 1989 Lattice-dynamical calculation of the Kapitza resistance between fcc lattices *Phys. Rev.* B **40** 3685–93
[13] Konatham D, Papavassiliou D V and Striolo A 2012 Thermal boundary resistance at the graphene–graphene interface estimated by molecular dynamics simulations *Chem. Phys. Lett.* **527** 47–50
[14] Hu L, Desai T and Keblinski P 2011 Thermal transport in graphene-based nanocomposite *J. Appl. Phys.* **110** 33517
[15] Mao R, Kong B D, Kim K W, Jayasekera T, Calzolari A and Nardelli M B 2012 Phonon engineering in nanostructures: controlling interfacial thermal resistance in multilayer-graphene/dielectric heterojunctions *Appl. Phys. Lett.* **101** 113111
[16] Chen Y, Jayasekera T, Calzolari A, Kim K W and Nardelli M B 2010 Thermoelectric properties of graphene nanoribbons, junctions and superlattices *J. Phys.: Condens. Matter* **22** 372202
[17] Shenogina N, Godawat R, Keblinski P and Garde S 2009 How wetting and adhesion affect thermal conductance of a range of hydrophobic to hydrophilic aqueous interfaces *Phys. Rev. Lett.* **102** 156101
[18] Balandin A A 2011 Thermal properties of graphene and nanostructured carbon materials *Nature Mater.* **10** 569–81
[19] Pop E, Varshney V and Roy A K 2012 Thermal properties of graphene: fundamentals and applications *MRS Bull.* **37** 1273–81
[20] Shi L 2012 Thermal and thermoelectric transport in nanostructures and low-dimensional systems *Nanoscale Microscale Thermophys. Eng.* **16** 79–116
[21] Sadeghi M M, Pettes M T and Shi L 2012 Thermal transport in graphene *Solid State Commun.* **152** 1321–30
[22] Zhang C, Zhao W, Bi K, Ma J, Wang J, Ni Z, Ni Z and Chen Y 2013 Heat conduction across metal and nonmetal interface containing imbedded graphene layers *Carbon* **64** 61–6
[23] Cai W, Moore A L, Zhu Y, Li X, Chen S, Shi L and Ruoff R S 2010 Thermal transport in suspended and supported monolayer graphene grown by chemical vapor deposition *Nano Lett.* **10** 1645–51
[24] Koh Y K, Bae M-H, Cahill D G and Pop E 2010 Heat conduction across monolayer and few-layer graphenes *Nano Lett.* **10** 4363–8
[25] Mak K F, Lui C H and Heinz T F 2010 Measurement of the thermal conductance of the graphene/SiO_2 interface *Appl. Phys. Lett.* **97** 221904
[26] Shenogin S 2004 Role of thermal boundary resistance on the heat flow in carbon-nanotube composites *J. Appl. Phys.* **95** 8136
[27] Brenner D W, Shenderova O A, Harrison J A, Stuart S J, Ni B and Sinnott S B 2002 A second-generation reactive empirical bond order (REBO) potential energy expression for hydrocarbons *J. Phys.: Condens. Matter* **14** 783
[28] Yi P and Rutledge G C 2011 Molecular simulation of bundle-like crystal nucleation from n-eicosane melts *J. Chem. Phys.* **135** 24903
[29] Wei D, Song Y and Wang F 2011 A simple molecular mechanics potential for μm scale graphene simulations from the adaptive force matching method *J. Chem. Phys.* **134** 184704
[30] Plimpton S 1995 Fast parallel algorithms for short-range molecular dynamics *J. Comput. Phys.* **117** 1–19
[31] Wei Z, Ni Z, Bi K, Chen M and Chen Y 2011 Interfacial thermal resistance in multilayer graphene structures *Phys. Lett.* A **375** 1195–9
[32] Ni Y, Chalopin Y and Volz S 2012 Calculation of inter-plane thermal resistance of few-layer graphene from equilibrium molecular dynamics simulations *J. Phys.: Conf. Ser.* **395** 12106
[33] Lemmon E W, McLinden M O and Friend D G *Thermophysical Properties of Fluid Systems* (*NIST Standard Reference Database No 69*) (Gaithersburg, MD: NIST)
[34] Neek-Amal M and Peeters F M 2011 Lattice thermal properties of graphane: thermal contraction, roughness, and heat capacity *Phys. Rev.* B **83** 235437
[35] Tikhonov K S, Sinova J and Finkel'stein A M 2013 Spectral non-uniform temperature and non-local heat transfer in the spin Seebeck effect *Nature Commun.* **4** 1945
[36] Alley W E and Alder B J 1983 Generalized transport coefficients for hard spheres *Phys. Rev.* A **27** 3158
[37] del-Castillo-Negrete D 2010 Non-diffusive, non-local transport in fluids and plasmas *Nonlinear Process. Geophys.* **17** 795–807
[38] Mahan G D and Claro F 1988 Nonlocal theory of thermal conductivity *Phys. Rev.* B **38** 1963
[39] Chen G 1996 Nonlocal and nonequilibrium heat conduction in the vicinity of nanoparticles *J. Heat Transfer* **118** 539–45